Academic Journal of Science and Technology
ISSN: 2771-3032 | Vol. 10, No. 3, 2024

Surface Elevation Change Monitoring Based on ICESat-2 Satellite Altimetry Data

Shuaikang Geng, Jinhua Lu

Henan Polytechnic University School of Geomatics and Land Information Engineering, Jiaozuo 454000, China

Abstract: The ICESat-2 (Ice, Cloud and Land Elevation Satellite-2), launched by NASA on September 18, 2018, offers higher precision in surface elevation monitoring. This study aims to investigate the surface elevation changes over different time periods in the Delong and Bulianta open-pit mines in Wulanmuren Township, Ordos City, using ICESat-2 laser data. The study utilizes the spatial distribution information of each photon from ATL03 (terrain elevation data) and the classification information of each photon from ATL08 (vegetation canopy height and surface elevation data) to extract surface photon elevation data for different periods in the same area. The precision of ICESat-2 satellite elevation data is validated using the on-board radar data from Henan Polytechnic University's Feima unmanned aerial vehicle D2000 in Jiaozuo City, Henan Province.Results indicate that in the No.1 area of the Delong open-pit mine, the surface subsided by approximately 16.3 meters between November 14, 2019, and November 10, 2021, due to soil removal operations. In the No.2 and No.3 areas of the Bulianta open-pit mine, the surface was uplifted by 3.1 meters and 13.6 meters, respectively, between May 16, 2019, and August 13, 2020, due to backfilling after mining. Additionally, the No.4 area was uplifted by about 10.5 meters between November 14, 2019, and November 10, 2021.Furthermore, the accuracy assessment yielded the following results: R2=0.956, RMSE=0.324, and MAE=0.105 meters, indicating that ICESat-2 data can be used as scientific data for inverting surface elevation changes.

Keywords: ICESat-2, ATL03, ATL08, surface elevation change.

1. Introduction

Surface elevation change is one of the essential indicators of Earth's surface, and it holds significant importance in understanding the dynamic changes and related environmental and climatic processes [1-2]. Changes in polar ice caps and glaciers, land crust movements, mining activities, and groundwater extraction can all lead to variations in ground elevation [3]. Local changes in glacier and ice cap elevations can directly affect local climates and hydrological cycles, and such changes can have severe destructive effects on buildings, underground pipelines, roads, bridges, and dams [4]. With human activities and natural processes increasingly impacting the Earth's surface, timely and accurate monitoring of surface elevation changes becomes crucial for understanding climate change, assessing natural disaster risks, managing water resources, and preserving the environment [5-6].With the continuous development of satellite technology, high-precision laser altimetry data provide new opportunities and breakthroughs for monitoring surface elevation changes [7]. Satellite-borne laser altimetry technology can achieve centimeter-level accuracy in generating Digital Terrain Models (DTMs) [8-9]. Using laser altimetry satellites, multiple temporal data of the same region can be acquired to understand ground elevation changes over time.

Since 2003, the National Aeronautics and Space Administration (NASA) has launched several laser altimetry-based Earth observation satellites, including the Ice, Cloud, and Land Elevation Satellite (ICESat) equipped with the Geoscience Laser Altimeter System (GLAS). ICESat's main mission was to monitor elevation changes in polar regions and Greenland ice sheets, providing valuable datasets for precise DEM (Digital Elevation Model) creation for polar ice sheets [10-11]. Subsequently, other laser altimetry satellites, such as the Global Ecosystem Dynamics Investigation (GEDI), GF-7, and ICESat-2 with the Advanced Topographic Laser Altimeter System (ATLAS), were launched for global Earth observation [12]. Researchers, including Wang, Nie, Lamsters, and others, have utilized ICESat/GLAS data to invert DTM of polar glaciers, showing a high correlation with measured values [12-15]. Chen Guodong and others have analyzed the elevation change trend of the Greenland ice sheet from June 2003 to October 2009 using ICESat laser altimetry data with a trend of -16.79±0.84 cm·year-1, indicating a slowdown in the rate of inland elevation accumulation above 2000 meters and an increasing trend of Greenland ice sheet melting [16]. Compared to the GLAS carried by the ICESat satellite, GEDI significantly improves spatial resolution. Yuan Zhihui and others verified the accuracy of ground elevation and canopy height extracted from GEDI data using airborne LiDAR data, indicating that correcting GEDI data's geolocation errors can significantly improve ground elevation accuracy [17]. Liu Lijuan and others compared six algorithms provided in GEDI L2A products to estimate ground elevation and found the selected optimal algorithm effectively improved the accuracy of ground elevation estimation [18]. However, ICESat/GLAS and GEDI still have certain limitations in obtaining high-resolution elevation changes of the same region at different times. The ICESat-2 with the ATLAS instrument, which adopts a multi-beam system and achieves a spatial resolution of 70 cm, provides photon-counting data, meaning that every photon event is marked with position and time. Therefore, studying ICESat-2 data for obtaining elevation changes of the same area at different times is of significant importance [19-22]. Huang Jiapeng and others used strong and weak beam data from ICESat-2/ATLAS to invert under-canopy DTM, showing that the strong beam had better inversion accuracy than the weak beam [19-20]. Zhu Jun and others discussed the impact of data acquisition time, vegetation coverage, terrain slope, and season on the accuracy of terrain data extracted from ICESat-2 ATL08 data [21]. Pang Shujian and others

used ICESat-2 laser height data, SRTM data, TerraSAR-X/TanDEM-X synthetic aperture radar, and other data to study the elevation changes of Malan Mountain Glacier from 2000 to 2020. The research indicated that the surface elevation change of 41 glaciers was -5.64±0.96 m, showing an obvious negative balance influenced by the increase in summer temperatures [22].

In summary, research on surface elevation changes based on laser altimetry data provides new perspectives and data support to deeply understand dynamic changes in the Earth's surface. To explore the inversion of surface elevation changes using ICESat-2/ATLAS data at different times in the same region, this study utilizes ATL03 and ATL08 data products as research objects for the study area.

2. Research Area and Data

2.1. Study Area

The Delong open-pit mine and the Bulianta open-pit mine are located in Wulanmuren Township, Yijinhuoluo Banner, Ordos City, Inner Mongolia Autonomous Region. The central coordinates of the mining areas are approximately (110°07′27″E, 39°23′43″N) for the Delong open-pit mine and (110°10′18″E, 39°21′02″N) for the Bulianta open-pit mine.The Ulanmulun coal mine dedicated coal transportation line runs from north to south through the mining areas, while the Bao-Shen railway and Bao-Fu highway pass through the town from north to south, providing convenient transportation conditions for the mining area.The climate in the mining area is classified as a semi-desert, semi-arid plateau continental climate. It experiences abundant sunshine, intense solar radiation, large diurnal temperature variations, cold winters, hot summers, and dry and windy springs and autumns.The terrain features of the mining area show the characteristics of a plateau erosion hilly landform, with the overall topography sloping from west to east, and an elevation ranging from 1180 to 1210 meters above sea level.The mining area is extensively covered by Quaternary aeolian sands and is classified as a semi-desert and desert region. The climate is characterized by a semi-desert, semi-arid plateau continental climate, with abundant sunshine and intense solar radiation. The diurnal temperature variation is significant. The annual precipitation ranges from 194.7 to 531.6 mm, and the annual evaporation is between 2297.4 to 2833.0 mm, which is 5 to 11 times the annual precipitation amount.

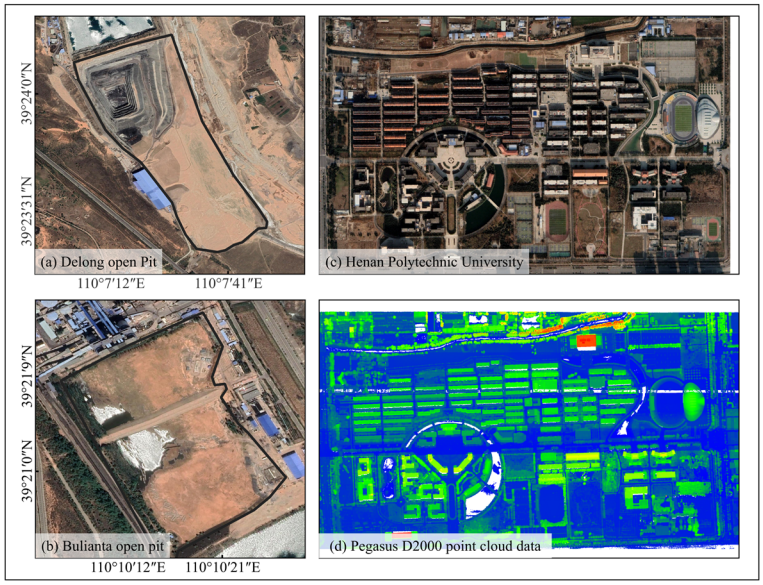

Figure 1. Research Area Overview

2.2. ICESat-2 Data Acquisition Modes

During its orbit around the Earth at a nominal altitude of about 500 km, the ICESat-2 satellite carries an Advanced Topographic Laser Altimeter System (ATLAS) that releases 104 laser pulses to the Earth's surface every second. Each laser pulse contains approximately 3 billion photons, but fewer than 60 photons are detected when they return to the photon telescope, as shown in Figure 2(a). Each pulse is split into six laser beams, creating footprints with a diameter of approximately 17 meters on the Earth's surface. The beams are arranged in three groups of six columns each, labeled as 1L(R), 2L(R), and 3L(R) from left to right. The distance between the groups is about 2.5 km, and within each group, the spacing is about 90 meters. Each group consists of one strong beam and one weak beam with an energy ratio of 4:1. The laser beams collect point cloud data every 0.7 meters along the track. ICESat-2 flight modes can be categorized into three types: forward, backward, and transition. The determination of the flight mode can be based on the "sc_orient" parameter in the ICESat-2 satellite data. In Figure (b), when the weak beam guides the strong beam (sc_orient=1), ICESat-2 is considered to be in the forward flight mode (along the ATLAS reference coordinate system +x direction), and the weak beam is positioned on the left side of the strong beam. In Figure (c), when the strong beam guides the weak beam (sc_orient=0), ICESat-2 is considered to be in the backward flight mode (along the ATLAS reference coordinate system -x direction), and the strong beam is positioned on the left edge of the weak beam. During the transition mode, which occurs when the direction of the strong and weak beams changes, the data collected by ICESat-2 is not processed.

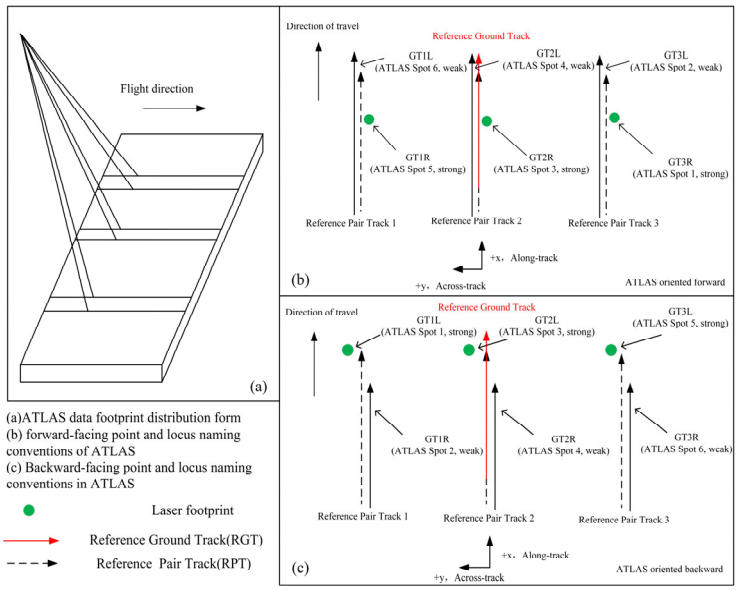

Figure 2. ICESat-2 Data acquisition mode

2.3. ICESat-2 Data

The National Snow and Ice Data Center (NSIDC) of the United States has released a total of 23 data products in HDF file format under four different levels (Level 1, 2, 3A, 3B) for the ICESat-2 mission. Each data product, ranging from ATL02 to ATL23, provides various information with different time coverage, time resolution, spatial coverage, and spatial resolution. Examples of these data products include ATL06 for Land Ice Height and ATL07 for Sea Ice Height, among others. Figure 3 illustrates the different levels of data products provided by ICESat-2.For research purposes, the ATL03 data product, Global Geolocated Photon Data, is used, which stores the spatial distribution information for each photon, including longitude, latitude, elevation, and geoid height correction. Another data product, ATL08, contains Land and Vegetation Height data, which classifies all photon events into categories such as canopy top photon, canopy photon, ground photon, and noise photon. Researchers can access the ATL03 and ATL08 data used in the study from the official website (https://nsidc.org/data/icesat-2/data). These datasets play a crucial role in understanding global ice and vegetation changes and are essential for various scientific investigations and environmental studies.

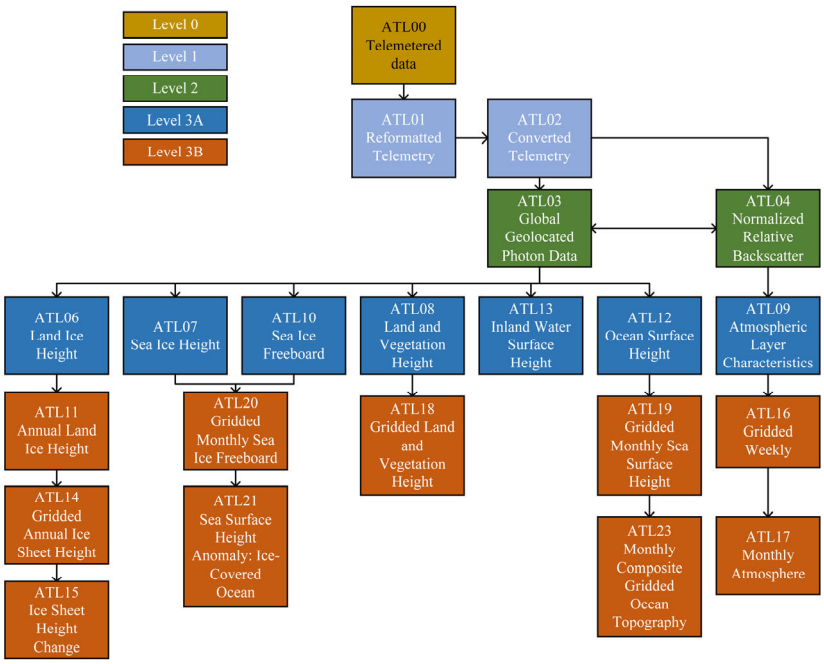

Figure 3. ICESat-2 Data Levels and Categories

2.4. FeiMa D2000 point cloud data

The objective of this research is to explore elevation changes in the same area at different time intervals. Although the publicly available data products from ICESat-2 can provide dense point cloud profiles, the accuracy of extracting surface elevation has not been fully validated. Hence, we utilized the FeiMa drone D2000 flight platform from Henan

Polytechnic University, equipped with the D-LiDAR2000 lightweight airborne LiDAR system, to collect LiDAR data and verify the accuracy of ICESat-2/ATLAS in extracting surface heights. As shown in Figure 1(c)(d), the images display the Google Earth imagery and drone imagery data from Henan Polytechnic University. The FeiMa D2000 drone is a quadcopter surveying UAV launched by Shenzhen FeiMa Robotics Technology Co., Ltd. in 2020. The drone has multiple functionalities, including carrying orthophoto cameras, oblique cameras, infrared sensors, video cameras, etc. It also has an adjustable flight height capability, allowing it to follow the terrain and maintain a consistent height above the ground. With a maximum flight ceiling of 6000 meters, it can conduct variable altitude flight operations in high-altitude and high-altitude difference areas. Additionally, the drone features full-automatic self-inspection without the need for magnetic compass calibration. Prior to flight, it performs self-checks of posture at a height of 1 meter from the ground and automatically takes off after confirming flight safety. Utilizing RTK+PPK fusion calculation technology, it ensures high-precision positioning, with take-off and landing point errors within 0.2 meters, achieving full-process operation without the need for a remote controller. The drone is equipped with FeiMa's self-developed D-LiDAR2000 LiDAR, which utilizes lightweight, long-range, and high-precision laser sensors. Combined with FeiMa's high-precision integrated navigation product and the drone manager data settlement and fusion algorithm, the FeiMa D-LiDAR2000 can achieve a measurement accuracy of 5 cm at a flight altitude of 50 meters. Through these technologies and equipment, we can obtain high-precision UAV LiDAR data to verify and complement the accuracy information of ICESat-2/ATLAS data products in surface elevation extraction.

3. Research Methodology

To explore the surface elevation changes in the same area at different times using ATLAS laser beams, the study selected and processed the ATL03 and ATL08 data. The specific steps involved are as follows:

(1) Point cloud denoising is the primary and crucial step in processing ICESat-2 laser altimeter satellite ATL03 point cloud data. The study utilized the Differential, Regressive, and Gaussian Adaptive Nearest Neighbor (DRAGSNN) algorithm provided in the ICESat-2 online Algorithm Theoretical Basis Document to denoise the data. Considering that the study area is semi-desert and desert regions with less than 5% vegetation coverage and relatively flat terrain, the researchers successfully eliminated the influence of the DRAGSNN algorithm's inability to effectively extract weak surface signal points under dense vegetation cover.

(2) Based on the shapefile of the open-pit mine boundary and the kml file of the ICESat-2 laser trajectory, the overlapping area was selected as the study area, as shown in Figure 4.

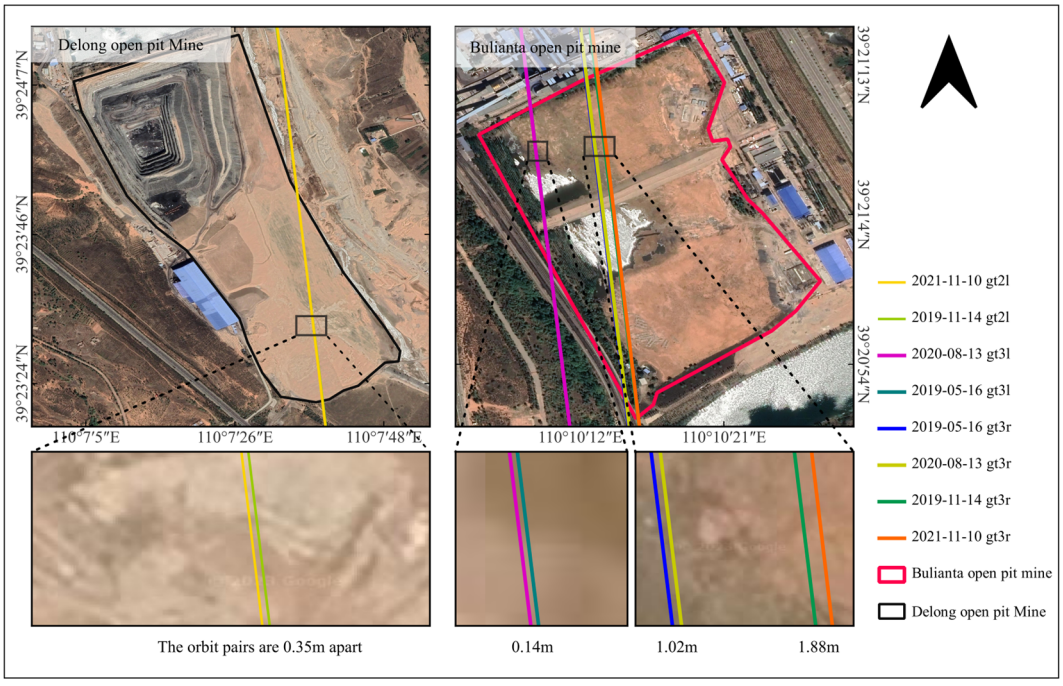

Figure 4. Schematic diagram of ICESat-2 laser orbit

(3) Extracted parameters for each laser point cloud data passing through the study area include longitude (lat_ph), latitude (lon_ph), elevation (h_ph), and elevation corrected to the geoid (geoid) in the WGS84 coordinate system. The parameters involved in the study are listed in Table 1.

(4) Simultaneously obtaining the spatial distribution and classification information of each photon is a critical task that requires association based on the indexing methods of ATL03 and ATL08 data. In ATL03, each photon has two indexing methods: one is sequentially numbered according to the GPS time of photons, known as photon ID, and these records are stored in (Group: /gtx/heights). The other method groups photons every 20 meters along the track, and each group is sequentially numbered, known as segment ID, stored in (Group: /geolocation/segment_id), and the starting photon ID for each group is stored in (Group: /geolocation/ph_index_beg). In ATL08, statistics are made in approximately 100-meter segments along the track. The photons within each segment are recorded using ATL03's second indexing method, i.e., each photon's segment ID is

stored in (Group: /gtx/signal_photons/ph_segment_id), and the relative index within the group is stored in (Group: /gtx/signal_photons/classed_pc_indx). To associate photon information, researchers need to traverse all photons in both ATL03 and ATL08 and match the corresponding segments using the parameter (ph_segment_id=segment_id). This allows obtaining the photon ID of all ATL08 photons in ATL03, using the following calculation formula: classed_pc_indx + ph_index_beg-1. Subsequently, by linking the longitude, latitude, and other information from ATL03 data with the obtained photon ID, the complete spatial distribution and classification information of each photon can be acquired. This ensures reliable data foundation for subsequent analysis and research.

(5) The official NASA classification algorithm categorizes point cloud data into noise photons, ground photons, canopy photons, and canopy top photons, and this information is stored in the classification parameter (class_pc_flag). The study extracted class_pc_flag=1, which represents the surface photons under investigation.

Table 1. Data sources.

Parameter	Description of parameters	Source of parameters
Lat_ph	Latitude of each received photon	ATL03/gtx/heights/lat_ph
Lon_ph	Longitude of each received photon	ATL03/gtx/heights/lon_ph
h_ph	Height of each received photon	ATL03/gtx/heights/h_ph
sc_orient	This parameter tracks the spacecraft orientation between forward,backward and transitional flight modes	ATL03/orbit_info /sc_orient
geoid	Geoid height above WGS-84 reference ellipsoid	ATL03/gtx/geophys_corr /geoid
Segment_id	A7digit number identifiying the along-track geolocation segment number	ATL03/gtx/geolocation /segment_id
ph_index_beg	Index (1-based) within the photonrate data of the first photon within this segment	ATL03/gtx/geolocation/ ph_index_beg
classed_pc_flag	Land vegetation ATBD classification flag for each photon as either noise, ground, canopy,and top of canopy. 0=noise, 1=ground, 2=canopy, or 3=top of canopy	ATL08/gtx/signal_photons/classed_pc_flag
classed_pc_indx	Index (1-based) of the ATL08 classified signal photon from the start of the ATL03 geolocation segment specified on the ATL08 product at the photon rate in the corresponding parameter, ph_segment_id,ph_segment_id	ATL08/gtx/signal_photons/classed_pc_indx
ph_segment_id	Segment ID of photons tracing back to specific 20m segment_id on ATL03	ATL08/gtx/signal_photons/ph_segment_id

4. Results and Analysis

Through the processing of ATL03 and ATL08 data, we obtained the surface elevation changes of Delong Open-pit Mine Dump and Bulianta Open-pit Mine at different times, as shown in Figure 5(a)(b). In Zone 1, Google Earth historical images from November 14, 2019, and May 18, 2021, show significant changes in Delong Open-pit Mine Dump. In April 2018, the northern part of the Delong Open-pit Mine was almost fully excavated, requiring cleanup of the southern dump. By June 2021, the topsoil of the dump had been completely cleared. Based on visual analysis of Figure 5(b) on May 18, 2021, the terrain in Zone 1 appeared flat, and the laser tracks from the two time periods in Figure 4 were approximately 0.35m apart. Therefore, we can consider the surface elevation on November 10, 2021, to be equivalent to the elevation of the gt2l track on November 10, 2021. In Figure 6(a), the surface elevations in Zone 1 for the two periods are 1128.4m and 1112.1m, respectively, indicating a subsidence of approximately 16.3m.

Regarding Bulianta Open-pit Mine, the mining operation was completed before May 2019, followed by backfilling until June 2021. Figure 5(c)(d)(e) shows the Google Earth historical images for three time periods: July 7, 2019, August 11, 2020, and May 18, 2021. Combined with Figure 4, we can see that the laser tracks for Zone 2 from the two periods are approximately 0.14m apart, and the terrain appeared flat in the historical image on August 11, 2020. Thus, we can consider the surface elevation on August 13, 2020 (gt2l track), equivalent to the elevation of the gt2l track on May 16, 2019. In Figure 6(b), the surface elevations in Zone 2 for the two periods are 1082.2m and 1085.3m, indicating an elevation increase of approximately 3.1m.For Zone 3, a similar approach was used, considering the surface elevation on August 13, 2020 (gt3 track), to be equivalent to the elevation of the gt3r track on May 16, 2019. In Figure 6(c), the surface elevations for the two periods are 1072.3m and 1085.9m, indicating an elevation increase of approximately 13.6m in Zone 3 during the period from May 16, 2019, to August 13, 2020.In Zone 4, the distance between the laser tracks on November 14, 2019 (gt3r) and November 10, 2021 (gt3r) is the greatest, reaching 1.88m. However, based on historical Google Earth images, the terrain in this area appeared flat after backfilling was completed before June 2021. Therefore, the 1.88m difference in laser tracks has little impact on the elevation of the gt3r track on November 10, 2021, compared to the gt3r track on November 14, 2019. In Figure 6(d), the surface elevations for the two periods are 1081.8m and 1091.6m, indicating an elevation increase of approximately 10.5m in Zone 4 from November 14, 2019, to November 10, 2021.Through the above analysis, we have obtained the surface elevation changes in Delong Open-pit Mine Dump and Bulianta Open-pit Mine at different times.

Figure 5. Historical images of the study area

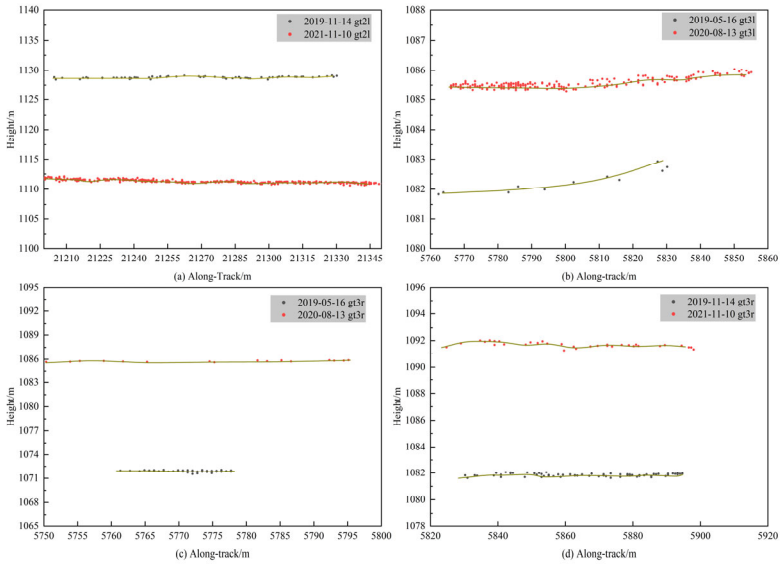

Figure 6. Schematic diagram of surface elevation change

5. Accuracy Evaluation

To investigate the accuracy of ATLAS laser point cloud in retrieving surface elevation, the study area selected was Henan Polytechnic University in Jiaozuo City, Henan Province, China. The validation data used for comparison were airborne LiDAR data collected by the D-LiDAR2000 module onboard the Feima D2000 unmanned aerial vehicle and the ICESat-2 point cloud data passing through the area on December 1, 2019.

The main purpose of this study was to analyze the accuracy of surface elevation inversion using ICESat-2 satellite laser data. Therefore, the first step involved separating the Feima D2000 airborne LiDAR data into ground and non-ground points. To achieve this, we utilized the CSF (Cloth Simulation Filter) filtering algorithm, a built-in feature in the CloudCompare point cloud processing software, to separate the airborne LiDAR data into ground and non-ground points. While preserving the original point cloud data characteristics, we effectively reduced the data volume of ground points by subsampling and thinning the non-ground points. Figure 7 displays the overlapping illustration of ground points obtained after applying the CSF filtering algorithm and the native algorithm of CloudCompare with the ICESat-2 laser track.

Through this processing, we obtained precise ground point cloud data, which we then compared with the ICESat-2 laser track to evaluate the accuracy of ATLAS laser point cloud in retrieving surface elevation.

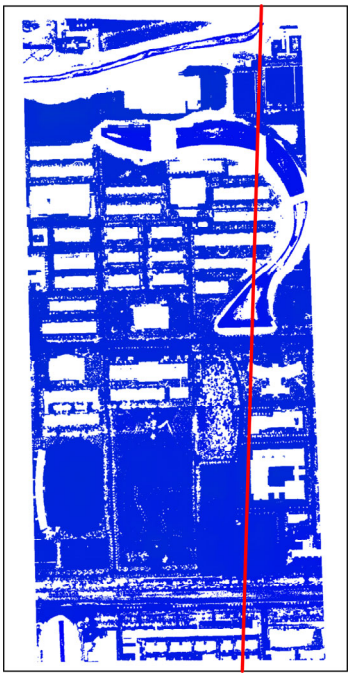

Figure 7. Schematic diagram of validation data research area

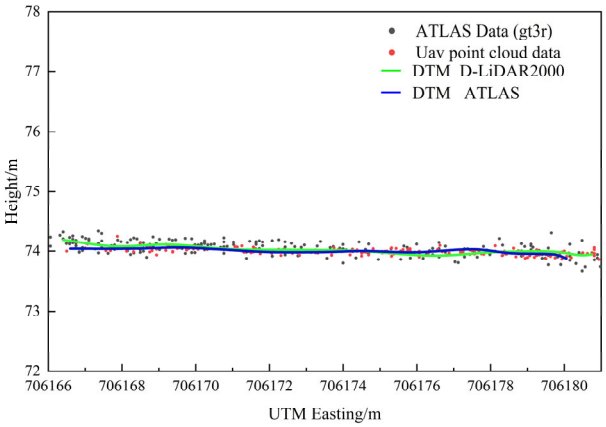

Figure 8. Surface inversion diagram of ATLAS and Pegasus D2000 data ICESat-2

In the third section of the article, the ICESat-2 laser point cloud data was processed, resulting in ground points for the Henan Polytechnic University area. Then, the overlapping area with the ICESat-2 track was extracted from the unmanned aerial vehicle (UAV) data. Figure 8 illustrates the terrain generated by the Feima D2000 airborne LiDAR data after cropping to match the ICESat-2 track. The blue line represents the Digital Terrain Model (DTM) generated from the ground points extracted from the ATL03 data after denoising and classification, while the green line represents the DTM generated from the Feima D2000 airborne LiDAR data.For a quantitative assessment of the relationship between the two datasets, the researchers conducted experiments and calculated the Root Mean Square Error (RMSE), Mean Absolute Error (MAE), and the Coefficient of Determination (R2). Figure 9 displays the scatter plot of the ICESat-2 data against the Feima D2000 data. The experimental results show R2=0.954, RMSE=0.324m, and MAE=0.105m. These results indicate a high consistency between the surface elevation retrieved from the ICESat-2 data and the one generated from the Feima D2000 airborne LiDAR data, confirming the height consistency between the two datasets.

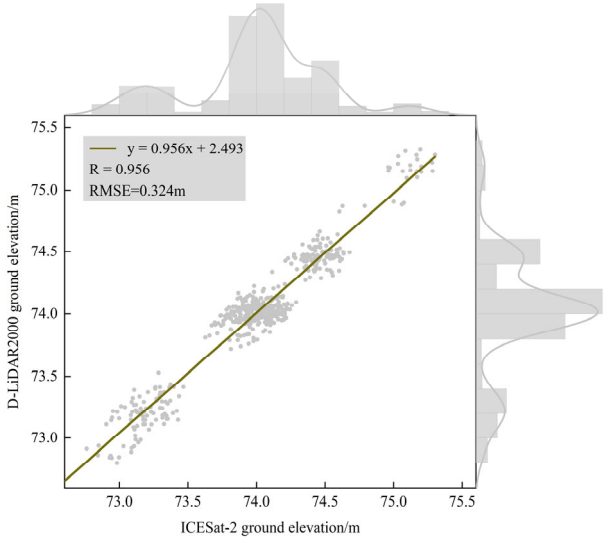

Figure 9. Scatter diagram of ICESat-2 data and Pegasus D2000 data

Therefore, the conclusion can be drawn that ICESat-2 data is a reliable scientific resource and can be used for studying surface elevation changes. This research finding demonstrates that the ICESat-2 laser point cloud data exhibits excellent accuracy in extracting surface elevation, providing robust data support for scientific research. The implications of this study are significant for gaining a deeper understanding of surface elevation changes and applications in environmental monitoring and resource management. The accuracy evaluation results presented here demonstrate the potential and reliability of ICESat-2 laser point cloud data in extracting surface elevation changes. These findings have important implications for various fields, including environmental monitoring and resource management, and provide valuable data for further research and decision-making.

6. Conclusion

In order to investigate the surface elevation changes in the same area at different times using ICESat-2/ATLAS data, we selected Delong Open-pit Mine Dump and Bulianta Open-pit Mine in Wulanhulun Town, Ordos City, as our study areas and used ATL03 and ATL08 data for elevation change analysis. The results of our study are as follows: In Zone 1 of Delong Open-pit Mine Dump, the surface experienced a subsidence of approximately 16.3 meters during the period from November 14, 2019, to November 10, 2021. In Zones 2 and 3 of Bulianta Open-pit Mine, the surface elevation rose by approximately 3.1 meters and 13.6 meters, respectively, during the period from May 16, 2019, to August 13, 2020. In Zone 4 of Bulianta Open-pit Mine, the surface elevation increased by approximately 10.5 meters during the period from November 14, 2019, to November 10, 2021. To assess the accuracy of ICESat-2 data in retrieving surface elevation, we used UAV-based airborne LiDAR data acquired by the Feima D2000 drone as validation data. The evaluation results showed good accuracy, with R2=0.956, RMSE=0.324 meters, and MAE=0.105 meters. This indicates that ICESat-2 data is reliable for generating surface elevation data and serves as a valuable source of scientific data. In conclusion, this study provides valuable insights into the surface elevation changes in the same area at different times through ATLAS inversion. In the future, NASA will continue the Lidar Surface Topography (LIST) mission [23-24], aimed at obtaining global land, vegetation, water, and glacier elevation data with a spatial resolution of 5 meters and an elevation resolution of 10 centimeters. This will further enhance our understanding of global landforms and environmental features.

References

[1] HUANG Hai-lan, WANG Zhengtao, Jin Tao-yong, et al. Determination of polar ice sheet elevation change using ICESat laser altimetry data [J]. Journal of Wuhan University (Information Science Edition)

[2] Ander Lang, Yang Jin, Wu Yongbin, et al. Research progress of ICESat-2 laser altimeter satellite [J]. Ocean Surveying and Mapping,2019,39(06):9-15.

[3] Li Qingshuo, Ke Changqing, Zhang Jie et al. Estimation of mass balance of Greenland Ice Sheet from 2003 to 2019 based on ICESat and ICESAT-2 laser altimetry data [J]. Journal of Geoinformation Science, 2002,24(03):558-571.

[4] Wan Jie, Liao Jingjuan, Xu Tao et al. Accuracy evaluation of SRTM data based on ICESat/GLAS altimeter data: A case study of the Tibetan Plateau [J]. Remote Sensing of Land and Resources,2015,27(01):100-105.

[5] Xie Dongping, LI Guoyuan, ZHAO Yanming et al. GEDI space-based laser altimeter system and its application [J]. International Space Science, 2018, No.480(12):39-44.

[6] Puliti S, Hauglin M, Breidenbach J,et al.Modelling above-ground biomass stock over Norway using national forest inventory data with ArcticDEM and Sentinel-2 data[J].Remote Sensing of Environment,2020,236:111501.

[7] Xie Dongping, LI Guoyuan, Wang Jianmin, et al. Application prospect of a new laser altimeter satellite ICESat-2 in geoscience [J]. Geomatics and Spatial Geographic Information, 2019,43(12):38-42+45.

[8] Ai H,Kentaro T, Ram A, et al.Synthesis of L-band SAR and forest heights derived from TanDEM-X DEM and 3digital terrain model for biomass mapping[J]. Remote Sensing, 2020, 12:349

[9] Ma Yue, Yang Fanlin, Wang Mingwei et al. Calculation of elevation change of Greenland Ice sheet using GLAS laser altimeter [J]. Infrared and Laser Engineering, 2015, 44(12): 3565-3569. (in Chinese)

[10] Li Guoyuan, Tang Xinming, Fan Wenfeng, et al. On-orbit geometric calibration of satellite laser altimeter using ground-based IR detector[J]. Infrare and Laser Engineering, 2017, 46(11): 1117004.(in chinese)

[11] Zhang Congkai, Yu Ying. Verification of accuracy of inversion of ground elevation and vegetation canopy height in ICESat-2/ATLAS data [J]. Forest Engineering, 2019,39(03):1-11.

[12] Wang Xianwei,David M Holland, Gudmundsson G. Hilmar, et al. Accurate coastal DEM generation by merging ASTER GDEM and ICESat/ GLAS data over Mertz Glacier, Antarctica[J]. Remote Sensing of Environment,2018,206:218-230.

[13] Wang Cheng, Dong Pinliang, Xi Xiaohuan,el al.A novel model for terrain slope estimation using ICESat/GLAS waveform data[J].IEEE Transactions on Geoscience and Remote Sensing,2018,50,1:217-227

[14] Lamster K,Karuss J,Krievans M,et al.High-resolution orthophoto map and digital surface models of the largest Argentine Islands (the Antarctic) from unmanned aerial vehicle photogrammetry[J]. Journal of Maps, 2020, 16(2):335-347.

[15] Guerra-Hernández J, Pascual A .Using GEDI lidar data and airborne laser scanning to assess height growth dynamics in fast-growing species: a showcase in Spain[J].Forest Ecosystems,2021,8(01):182-198.

[16] Chen Guodong, Zhang Shengjun. Determination of elevation and volume change of Greenland ice sheet using ICESat data [J]. Chinese Journal of Geophysics,2019,62(07):2417-2428.

[17] YUAN Huihui, Nie Sheng, Zhang Hebing et al. Accuracy evaluation and impact analysis of GEDI ground elevation and forest canopy height [J]. Remote Sensing Technology and Application,202,37(05):1056-1070. (in Chinese)

[18] Liu Lijuan, Wang Cheng, Nie Sheng et al. Analysis of effects of different GEDI L2A algorithms on ground elevation and forest canopy height accuracy [J]. Journal of University of Chinese Academy of Sciences, 2019,39(04):502-511.

[19] Huang Jiapeng, Xing Yanqiu, Qin Lei et al. Accuracy verification of ICESat-2/ATLAS data inversion of understory topography [J]. Infrared and Laser Engineering, 2020, 49(11):122-131. (in Chinese)

[20] HUANG Jiapeng, Xing Yanqiu, Qin Lei et al. Research on the accuracy of photon cloud denoising algorithm in forest area under weak beam conditions [J]. Transactions of the Chinese Society for Agricultural Machinery, 2019,51(04):164-172.

[21] Zhu Jun, Yang Panfeng, Li Yi, et al. Accuracy verification of ICESat-2 ATL08 terrain products: a case study of Spain [J]. Journal of Central South University,2022,29(01):226-238.

[22] Pang Shujian, Ke Changqing, Zhou Xinghua et al. Change of glacier mass balance in Malan Mountain by InSAR and LiDAR altiometry [J]. Journal of Remote Sensing, 2019,26(10):2094-2105.

[23] Krainak M A, Abshire J B, Camp J, et al. Laser transceivers for future NASA missions[J]. Proceedings of SPIE - The International Society for Optical Engineerin, 2012, 8381(8): 1-12.

[24] Yu A W, Krainak M A, Harding D J, et al. Development effort of the airborne lidar simulator for the lidar surface topography (LIST) mission[C]. 2011: 8182-8182.